

Processing the Attenuated Atmospheric Backscatter Profiles from the Measurements of the CO₂ Sounder Lidar in the 2017 ASCENDS/ABoVE Airborne Campaign

Paul T. Kolbeck
University of Maryland
kolbeckpaul@gmail.com

Xiaoli Sun
NASA Goddard Space Flight Center, Code 698
xiaoli.sun-1@nasa.gov

Revision C, 10/18/2020

Introduction

This report summarizes the algorithm and data processing used to obtain the attenuated atmospheric backscatter profiles measured by the pulsed CO₂ Sounder lidar developed by the NASA Goddard Space Flight Center (GSFC) [1] and deployed during the 2017 ASCENDS/ABoVE airborne campaign [2]. The algorithm produces time resolved attenuated backscatter profiles at the 1572 nm laser wavelengths along the same atmospheric column where the column CO₂ mixing ratios (XCO₂) [3] were measured. It provides a new data product from the CO₂ lidar measurement in addition to the XCO₂ measurements.

The CO₂ Sounder lidar measures in the wavelength region of the 1572.335 nm CO₂ absorption line [1]. The lidar's laser is stepped through 30 wavelengths across the absorption line at a rate of about 300 scans per second. The pulse energy of the ground returns attenuated by the CO₂ are used to determine the atmospheric XCO₂. The lidar has been successfully used in several airborne campaigns and measured XCO₂ with a standard deviation of about 0.7 parts per million (ppm) over a 1-second integration time [1][2]. In addition to the XCO₂ measurement, the lidar receiver also records the atmospheric backscattered signal strength continuously as the laser pulses propagates through the atmosphere. Preliminary results about the atmospheric backscattering profiles from the CO₂ Sounder lidar have been reported by Allan *et al.* (2018) [4]. In this project we completed the data processing by screening out outliers, correcting for all known instrument artifacts, and converting the raw lidar data to the product of the atmospheric backscattering cross section and the two-way atmosphere transmission, also known as attenuated backscatter profiles, in the nadir direction. These data provide additional information about the atmospheric scattering in the columns when the XCO₂ was measured. This report describes the algorithm used to convert the lidar measurement data into a data product showing the atmosphere backscattering profiles.

Level-0 Data Processing

The data from the CO₂ Sounder lidar were gathered continuously by the instrument and stored into a file at 1 second intervals. Each file contains 9 groups of pulses, each with 30 received pulse waveforms and their corresponding transmitted waveforms, one per wavelength, and averaged

over 32 repeated measurements. Figure 1 shows the laser wavelengths of the lidar and the CO₂ absorption line. Figure 2 shows a plot of the data from a 1-second data file in the unit of the waveform digitizer output (16-bit signed integers). The pulse waveforms are sampled at 10-ns intervals. Since the laser pulse rate is 10 KHz, the interval between pulses is 100,000 ns or 10,000 sample points. The dip in the pulse amplitudes in the middle of each 30-pulse group was caused by the CO₂ absorption by the atmosphere column from the lidar to the surface. The transmitted pulse waveforms were sampled at the same time interval but with only 1,000 sample points per pulse and they were concatenated and appended at the end of each group of 30 received pulse waveforms. Figures 3 and 4 display one group of the transmitted and the received pulse waveforms.

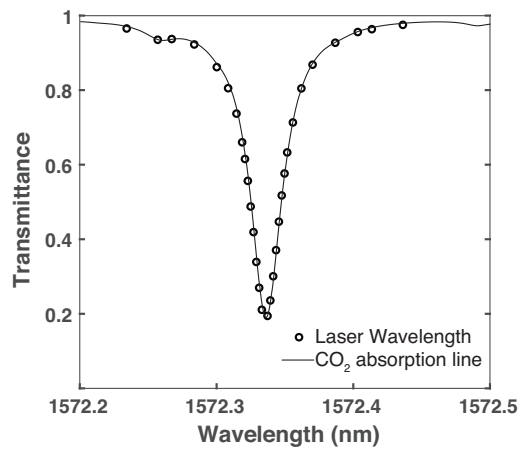


Figure 1. The laser wavelengths of the CO₂ Sounder lidar overlaid on the CO₂ absorption line near 1572.3 nm.

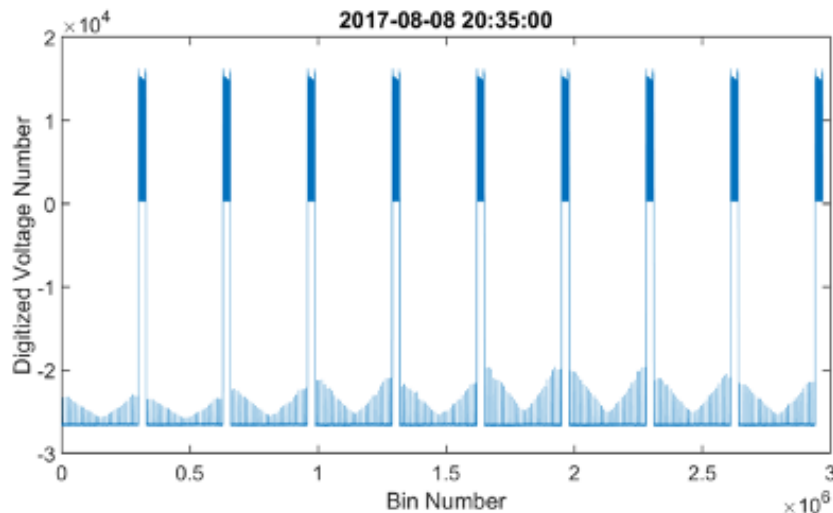


Figure 2. A plot of a 1-second lidar data in the raw data file. The lower regions display the atmosphere backscatter and ground return waveforms measured by the receiver, while the top regions display the corresponding transmitted waveforms.

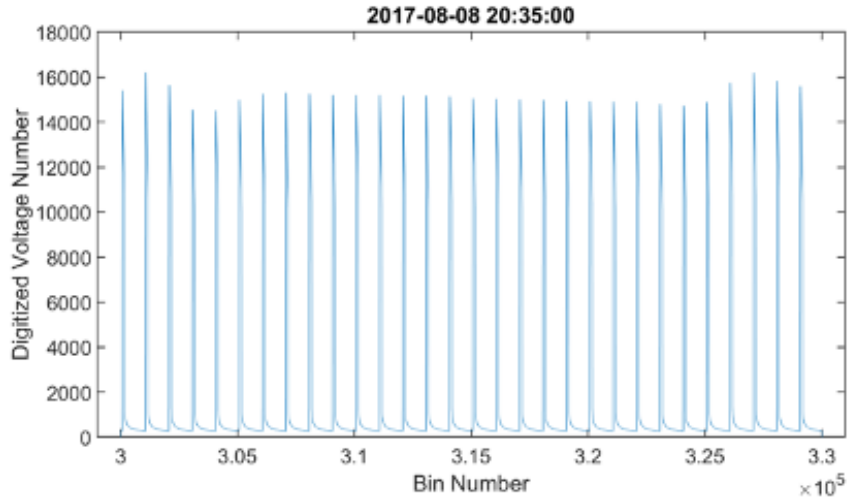


Figure 3: A zoomed in view of a section of the 30 transmitted waveforms from Figure 2. The laser is stepped in wavelength between each pulse. The amplitudes of the transmitted laser pulse waveform fluctuated by 5-10% and their effects on the measurement results are normalized out by dividing the received pulse energy by the transmitted ones.

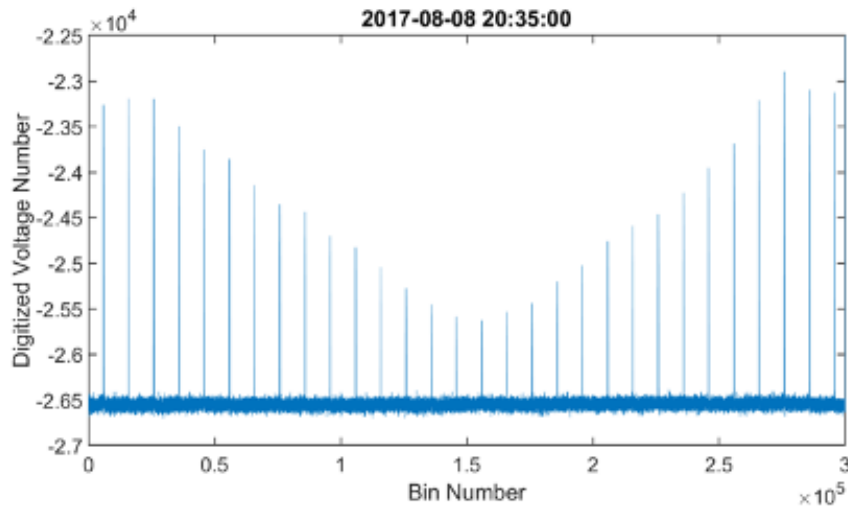


Figure 4: The 30 ground returns corresponding to the transmitted waveforms in Figure 3. The change in the amplitude of the ground returns with respect to the wavelength were caused by the CO₂ absorption.

The first level of processing takes each second of data and averages the measurement results at a number of selected off-line laser wavelengths across all nine groups of pulses. Here we averaged the signal amplitudes of wavelengths 2, 3, 4, 27, 28, 29 and 30, which were not significantly affected by the CO₂ absorption. For each of the wavelengths at each pulse, the DC offset is first estimated by calculating the average of a region immediately before the aircraft window return. Since the pre-window-return region is long after the ground return of the previous laser wavelength but before the next laser emission, it is composed primarily of the instrument noise plus a constant

DC offset. The DC offset is estimated by the mean of the waveform within this region and is subtracted from the following waveform. The transmitted pulse energies and their emission times are calculated from the area and the centroid of the transmitted pulse waveform. The received waveform is then normalized with respect to the corresponding transmitted pulse energies, and shifted up in time to the centroid times of the transmitted pulses. Following this, received pulse waveforms in the 1-second data file are averaged together to improve the signal to noise ratio (SNR). Finally, the averaged pulse waveform is converted into the unit of the detector output (millivolts) by dividing the waveform by the scale factor of the waveform digitizer to encompass a range of 1.25 volts, as shown in Figure 5.

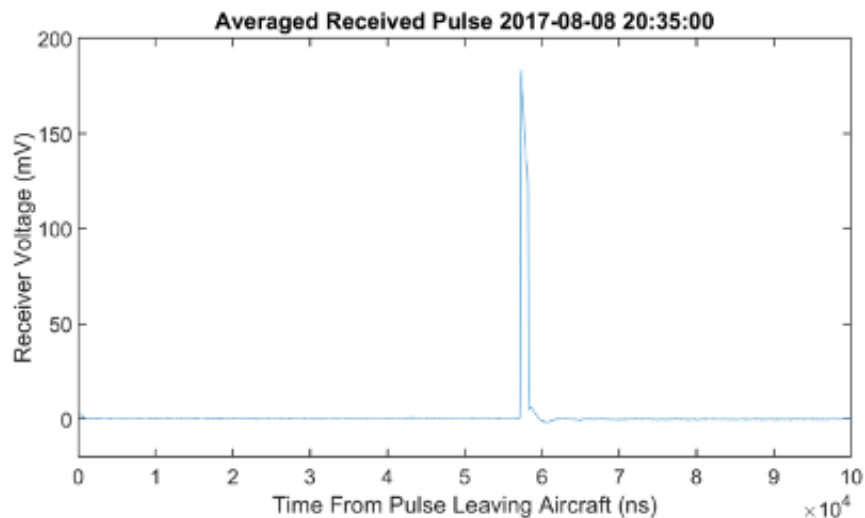


Figure 5: An example of a timepoint after each of the listed wavelengths in each of the pulses are normalized and averaged.

Data screening was performed to eliminate measurements that were made under poor conditions. The data records are omitted if they exhibit any of the following properties: the transmitted pulse waveforms are missing in the data file; saturated ground return pulse amplitudes which exceed a threshold value of 1.1 volts; data taken while the detector is still recovering from saturation with the estimated DC offset of the waveform below a minimum of 0 Volts or above a maximum of 0.5 Volts. Data points where the maximum and minimum of the ground return pulse amplitudes vary by more than 50% within the second are flagged. The mean and standard deviation of the waveform within the pre-window region for each averaged waveform as well as the average transmitted pulse energy over the entire flight are recorded.

Level-1 Data Processing

This level of data processing incorporates the aircraft's navigation data and converts the Level-0 data into attenuated backscatter cross section.

Alignment of the lidar data with the aircraft navigation data: The aircraft flight data are obtained from archived airborne campaign housekeeping data gathered during the flight. The following

parameters are extracted from the archived housekeeping data for each second: the UTC time from midnight on the day of the flight's beginning, the aircraft's latitude, longitude, altitude, pitch, and roll. The on-board radar also gave the height above the surface. The surface elevation is calculated as the difference between the aircraft GPS altitude and the lidar-measured height above the surface. Missing points in the surface elevation, e.g., cloud-obscured, are interpolated linearly based on the points bordering the missing region. The aircraft's latitude, longitude, altitude, pitch and roll are interpolated linearly only if certain conditions are met that make interpolation reasonable (e.g. small enough gap size and change in measured values). The archived housekeeping data is aligned in UTC time with the lidar data from Level-0 data processing.

Correction of lidar range offset and the effect of off-nadir pointing: For each time point, the following steps take place. If the lidar data shows a peak within 3 km below the aircraft that exceeds the average of the window return, the point is flagged, as this indicates near range cloud returns too close to the aircraft to be calibrated because the detector field of view did not completely overlap with the laser-illuminated region. The average pulse amplitude of the window return is recorded to calculate the detector gain for the laser pulse. The range offset from the laser emission to when the laser pulses leave the aircraft nadir window is corrected by shifting lidar waveform in time so that the beginning of the pulse waveform coincides with the aircraft window return.

Averaging: The waveforms are further averaged via a boxcar averaging window with the integration time equal to the transmitted laser pulse width (1 μ s). The data are then corrected for the effect of the aircraft roll and pitch angles by first dividing the sampling time by the cosine of the combined off-nadir pointing angle and then interpolating the resultant data at 15-meter intervals in the nadir direction. Then all data points in the waveforms above the aircraft altitude and below the ground return are removed. In the cases where there is no discernable ground return, points more than 200 m below the surface elevation are removed.

Scaling: The optical signal collected by the lidar can be written as

$$y(t) = \int_0^{\tau_L} x(\tau)h(t - \tau)d\tau$$

where $x(t)$ is the laser pulse shape and $h(t)$ is the impulse of the atmosphere, i.e. the ideal received optical signal when the laser pulse width is relatively short compare to the vertical resolution. In our case, the laser pulse width is relatively wide and the lidar signal is the convolution of the laser pulse width and the impulse response.

The impulse response is related to the volume atmospheric backscattering cross section by the lidar equation [5]

$$h(t) = E_{tx} \frac{c}{2} \frac{\beta[R(t)]}{\pi} T_a^2[R(t)] \frac{\eta_r A_{tel}}{R^2(t)} C_1$$

where E_{tx} is the transmitted laser pulse energy in joules, c is the speed of light, $\beta[r]$ is the atmosphere backscattering cross section at range r in the unit of m^{-1} (m^2 per unit volume m^3), $T_a^2[r]$ is the atmosphere transmission from the lidar to measurement range, η_r is the receiver

optical transmission, A_{tel} is the aperture area of the receiver telescope, $R^2(t)$ is the lidar range at time t after the laser pulse emission, and C_1 is the lidar detector responsivity in V/W.

The lidar signal out of the detector can be written as,

$$s(t) = C_1 \frac{c}{2\pi} \eta_r A_{tel} E_t \int_0^{\tau_L} x(\tau) \frac{\beta[R(t-\tau)] T_a^2[R(t-\tau)]}{R^2(t-\tau)} d\tau$$

with $x(t)$ the normalized laser pulse shape, i.e., $\int_0^{\tau_L} x(t) dt \equiv 1$, and τ_L is the laser pulse width.

The laser pulse can be approximated to have a rectangular shape, i.e.,

$$x(t) = \begin{cases} \frac{E_t}{\tau_L} & 0 \leq t \leq \tau_L \\ 0 & else \end{cases}$$

Assuming the atmospheric backscattering cross section and the transmission stay unchanged over the laser pulse interval (1 μ s, or 15 m in range), the lidar signal can be approximated as,

$$\begin{aligned} s(t) &\approx \frac{c}{2} \left(C_1 \eta_r A_{tel} \frac{E_t}{\pi} \right) \frac{1}{R^2(t)} \left[\frac{1}{\tau_L} \int_0^{\tau_L} \beta[R(t-\tau)] T_a^2[R(t-\tau)] d\tau \right] \\ &= \frac{c}{2} C_2 \frac{1}{R^2(t)} \langle \beta[R(t)] T_a^2[R(t)] \rangle \end{aligned}$$

where $C_2 = C_1 \eta_r A_{tel} \frac{E_t}{\pi}$ is a constant dependent solely of the instrument parameters. Therefore, the attenuated atmospheric backscattering cross section can be obtained from the lidar measurement by first multiplying the square of the lidar range and then a scale factor, as

$$\langle \beta[R(t)] T_a^2[R(t)] \rangle = C_3 [R^2(t) s(t)].$$

where $C_3 = 2/cC_2$ is the scaling factor. The left hand side of the above equation is the attenuated backscatter profile after converting time to altitude.

For the CO₂ Sounder lidar used in the 2017 airborne campaign, these instrument constants are

$$C_1 = \left(\eta_{det} G_{ApD} \frac{e_c}{h \lambda_{laser}} \right) Z_{TIA} G_{amp} \eta_{cable} \quad (\text{V/W})$$

$$C_2 = C_1 \eta_r A_{tel} \frac{E_t}{\pi} = C_1 \eta_r \frac{\pi \phi_{tel}^2}{4} (1 - L_{obs}) \frac{E_t}{\pi} \quad (\text{V m}^2 \text{ s})$$

where η_{det} is the detector quantum efficiency, G_{ApD} is the detector avalanche gain, e_c is the electron charge, h is Planck's constant, λ_{laser} is the laser wavelength, Z_{TIA} is the gain of the transimpedance preamplifier gain in V/W, G_{amp} is the post amplifier voltage gain, η_{cable} is the cable losses, ϕ_{tel} is the receiver telescope diameter and L_{obs} is the losses of the telescope aperture area due to the center obscuration.

Figure 6 shows a block diagram of the CO₂ lidar receiver, which shows how the incident optical signal is converted to the voltage signal recorded in the data files. Table 1 lists all the instrument parameter values needed to calculate these constants. The resultant detector responsivity is $C_1 =$

6.39×10^8 V/W for nominal APD gain, the instrument constant is $C_2 = 109$ V m² s, and the scaling factor to convert the range-corrected lidar measurement to attenuated atmospheric backscattering cross section is $C_3 = 6.12 \times 10^{-11}$ V⁻¹ m⁻³.

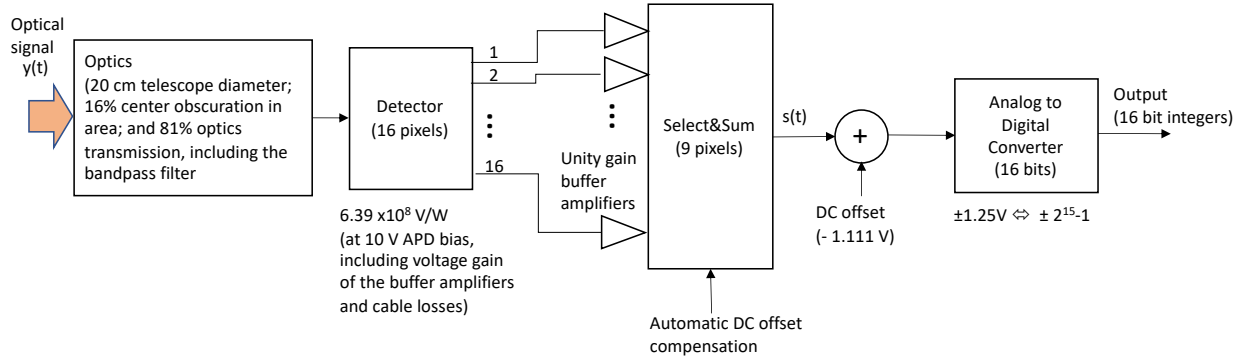


Figure 6: Block diagram of the CO₂ lidar receiver from the incident optical signal to the waveform digitizer output.

Table 1. Instrument Parameter Values of the CO₂ Sounder Lidar in 2017 Airborne Campaign [1]

Laser pulse energy, E_t	25 μ J
Laser pulse width, τ_L	1.0 μ s
Laser pulse rate	10 kHz
Laser wavelengths, λ_{laser}	1572.2 to 1572.5 nm
Telescope diameter, ϕ_{tel}	0.20 m
Telescope center obscuration, L_{obs}	16%
Receiver optical transmission, η_r	81.3%
Receiver field of view	500 μ rad
Receiver optical bandpass filter width	1.4 nm
Receiver integration time	1 s
Detector quantum efficiency, η_{det}	69.3%, including the effect of fill factor
Detector avalanche gain, G_{APD}	200 (10V bias)
Transimpedance amplifier gain, Z_{TIA}	320 kV/A
Post amplifier voltage gain, G_{amp}	12.6
Cable losses, η_{cable}	10%
Overall receiver responsivity* $(\eta_{det} G_{APD} / hc / \lambda_{laser}) Z_{TIA} G_{amp} (1 - \eta_{cable})$	$6.39e8$ V/W at 10 V APD bias, increase by about 2x for every 1 V increase in bias

* $h=6.626e-34$ m²kg/s is the Planck's constant

Multiplying the net signal waveforms by the square of the distance from the aircraft window and then by the scaling factor. Each waveform is now a vertical profile of the attenuated atmosphere backscatter cross section to the surface as shown in Figure 7.

Detector gain correction: The gain of the detector is corrected for by comparing the window returns throughout the flight. After filtering out anomalous window returns, which generally resulted from the aircraft flying through a cloud, the window returns are binned at an interval of

.01 mV. The bin with the maximum counts is used as a benchmark for a nominal gain of 1. Window returns close to 1/2 have a gain of 2, 1/4 a gain of 4, etc.

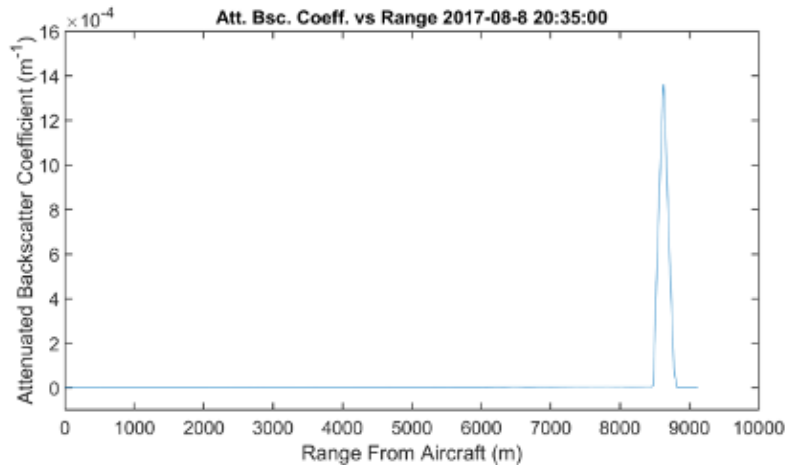


Figure 7: A typical 1-second atmospheric and surface backscattering profile after level 1 processing. The noise has been reduced considerably with the boxcar averaging.

Figure 8 shows the result of the atmosphere backscatter profile for a section of the flight on 8-8-2017. The log₁₀ of the attenuated backscatter coefficient is shown using a color scale and is plotted with respect to its time and altitude.

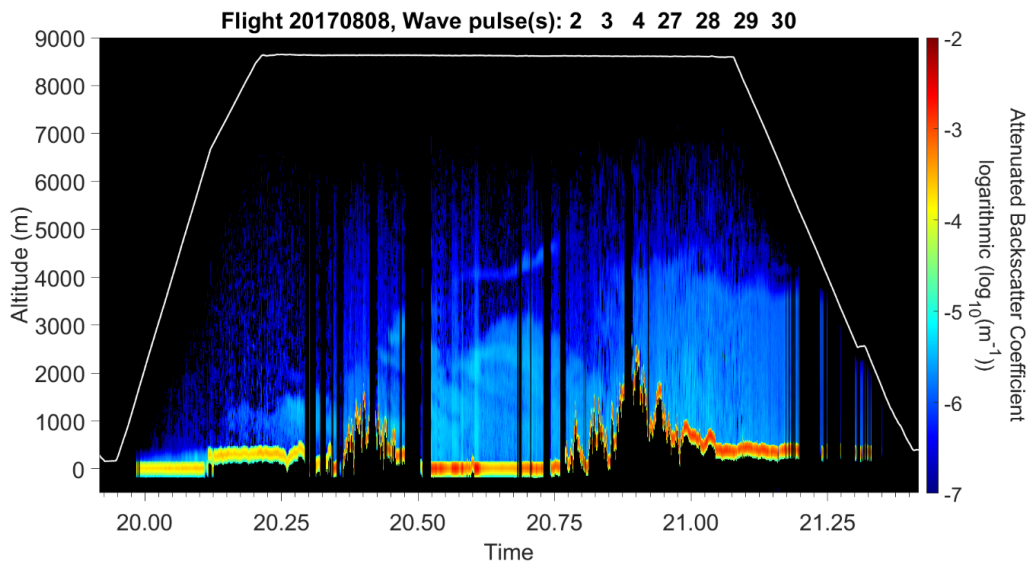


Figure 8: An example of atmospheric backscatter profiles for a section of the August 8, 2017 flight. The large peak indicating the ground return in Figure 5 can be seen as the orange band at the bottom of the plot.

The magnitudes of these results are similar to those reported by Spinhirne et al. (1997) [6] measured at 1.54 nm laser wavelength (note the difference in units, 1/m and 1/m/sr between the two). The vertical resolution is limited by the laser pulse width (1 μs), or 150 m, but with the signal

over-sampled at 15 m per point. The horizontal resolution along the aircraft ground track is the distance travelled by the aircraft in 1-s, or about 200 m. The profile can also be used to calculate the attenuated ground surface reflectance (product of the 2-way atmosphere transmission and the surface reflectance) by integrating the ground return portion of the profile. When the atmospheric transmission and surface reflectance are known, one can compare them with the lidar measurement to verify or refine the lidar calibration. For example, the lidar data over the desert over the Edwards Airforce base taken on 8-8-2017 gives an attenuated surface reflectance of 28%. This is close to the conditions estimates at the time for a 1-way atmospheric transmission of 80% and a desert diffuse surface reflectance of 45%.

The backscatter cross sections measured close to the aircraft are affected by the overlap factor of the lidar laser beam and the receiver field of view. The two start to partially overlap at a few hundreds of meters and becomes fully overlapped at 3-4 km [4]. Therefore, the backscatter cross sections measured are underestimated (and not calibrated) in this region.

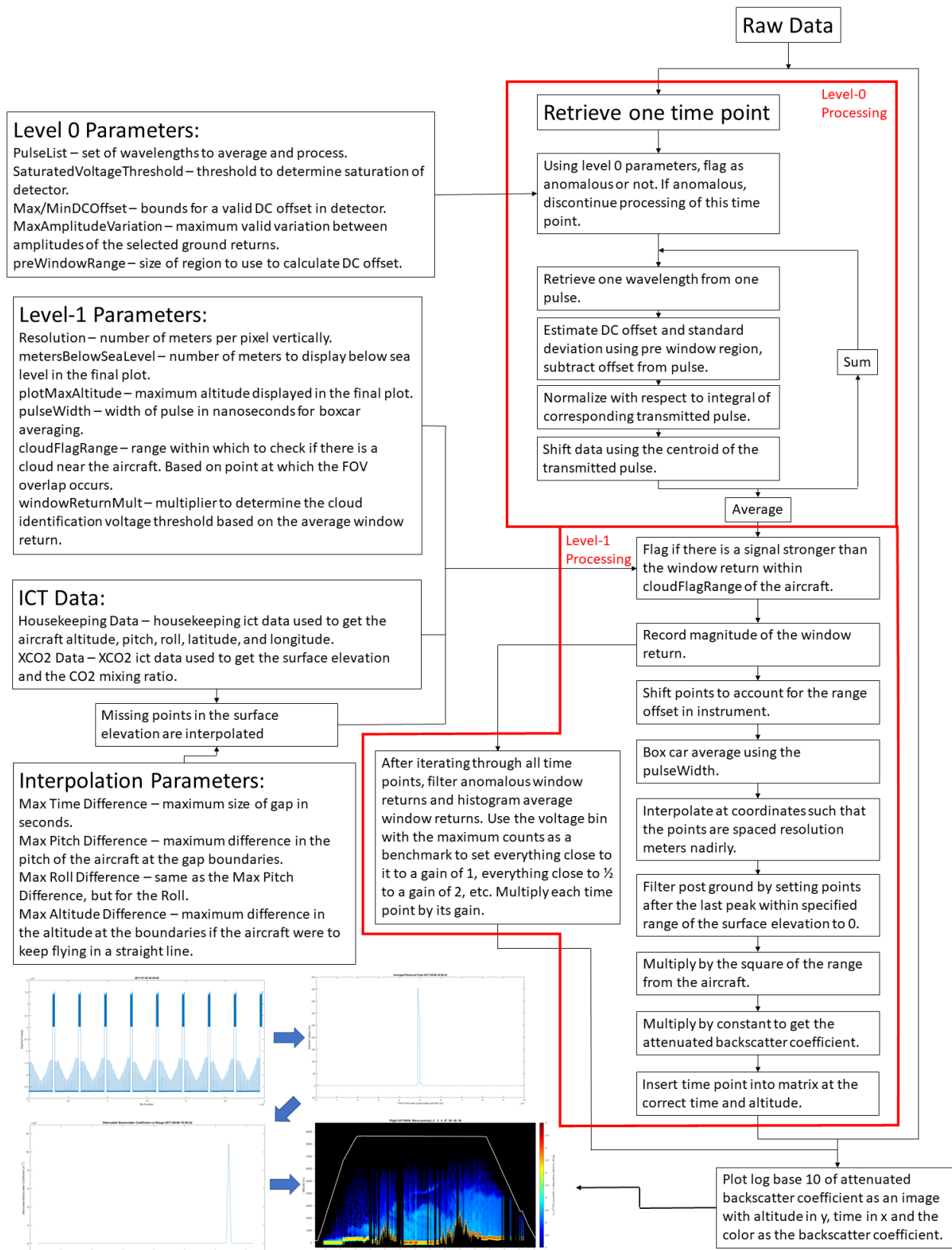
A flowchart of the data processing software is shown in Appendix A.

A set of summary plots of the attenuated backscatter profiles for all the 8 flights in 2017 are given in Appendix B. The horizontal axes of these plots are the time in second from the beginning of the data set, not the local or UTC time.

References

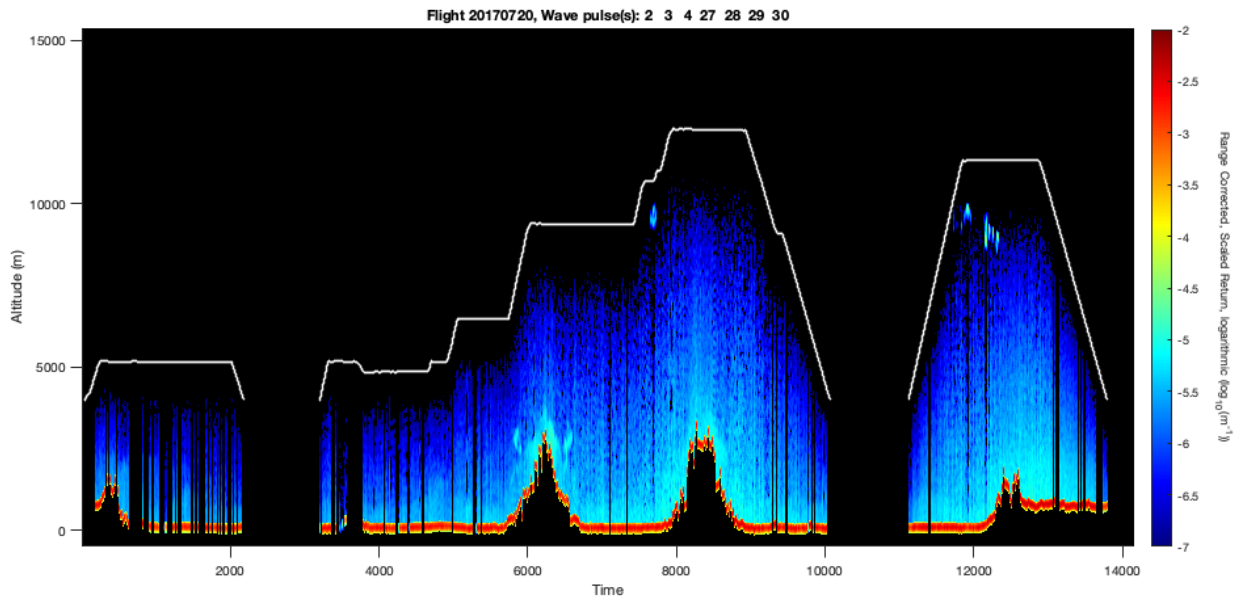
- [1] J. Abshire *et al.*, “Airborne measurements of CO₂ column concentrations made with a pulsed IPDA lidar using multiple-wavelength-locked laser and HgCdTe APD detector,” *Atmospheric Measurement Techniques (AMT)* Vol. 11, 2001-2025, 2018.
- [2] J. B. Abshire *et al.*, “Pulsed multiwavelength lidar measurements of CO₂ column concentrations in the 2017 ASCENDS airborne campaign,” *2018 Fall AGU Annual Meeting*, Washington DC, Dec. 10-14, 2018, Paper 31P-3156.
- [3] <https://www-air.larc.nasa.gov/cgi-bin/ArcView/ascends.2017>
- [4] G. Allan *et al.*, “Lidar measurements of CO₂ column concentrations in the Arctic region of North America from the ASCENDS 2017 airborne campaign,” *Proc. SPIE*, Vol. 10779, 1077906, 2018.
- [5] R. M. Measures, *Laser Remote Sensing: Fundamental and Applications*, Wiley, 1984
- [6] J. D. Spinhirne *et al.*, “Aerosol and cloud backscatter at 1.064, 1.54, and 0.53 μm by airborne hard-target-calibrated Nd:YAG/methane Raman lidar,” *Appl. Opt* **36**(15), 3475-3489, 1997.

Appendix A. Flow Chart of the Data Processing Software

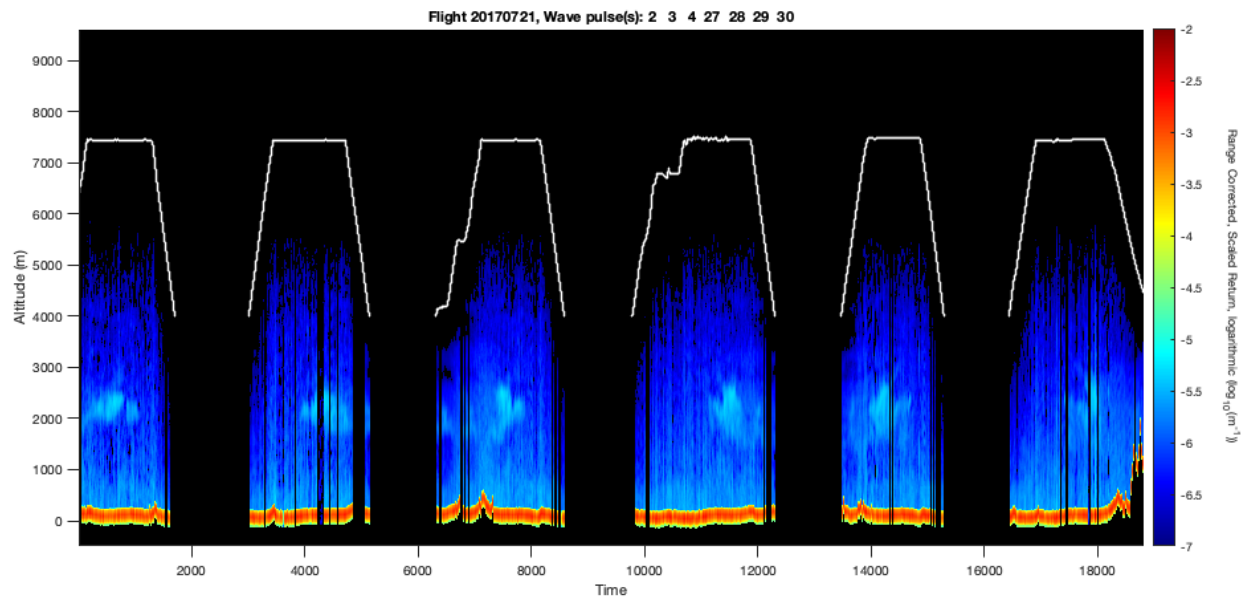


Appendix B. Summary Plots of the Attenuated Backscatter Profiles from the 2017 Airborne Campaign

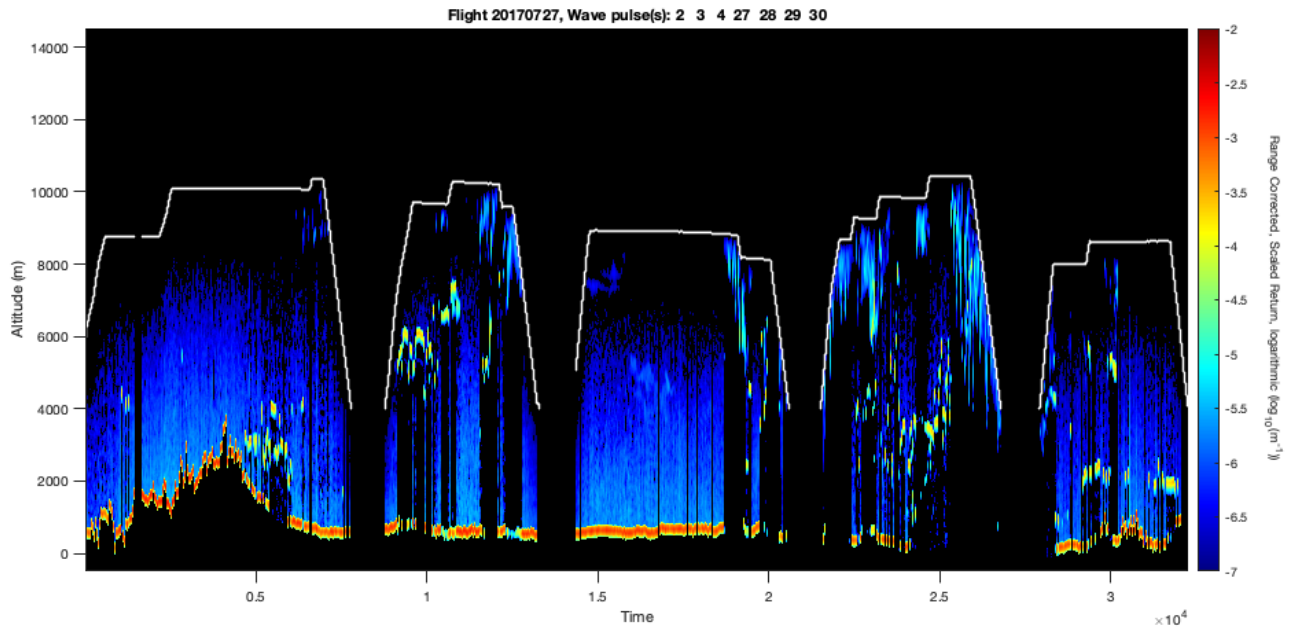
1. Engineering Flight, 7/20/2017



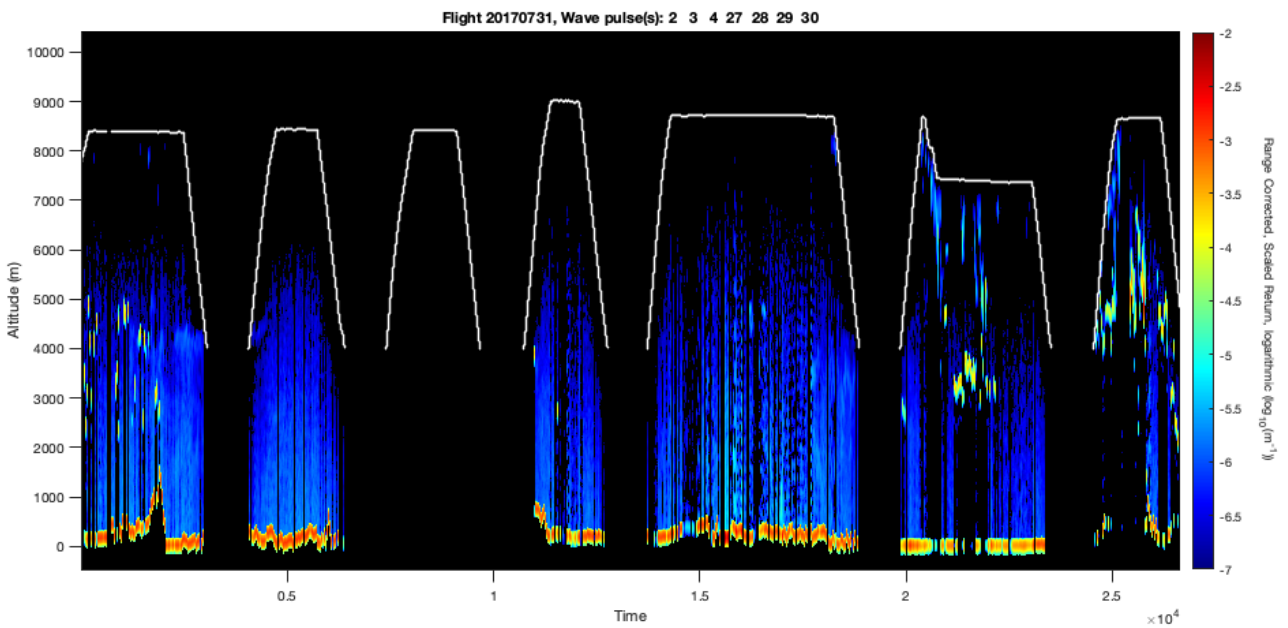
2. Calibration Flight, 7/21/2017



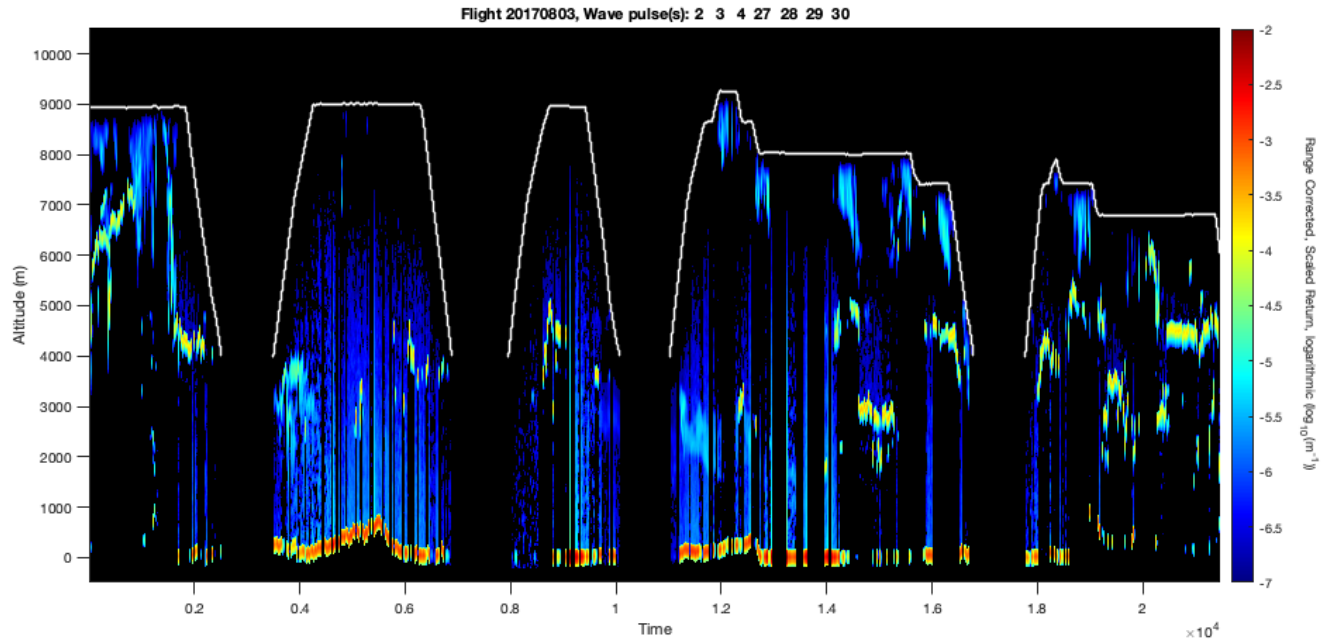
3. Science Flight 1, 7/27/2017



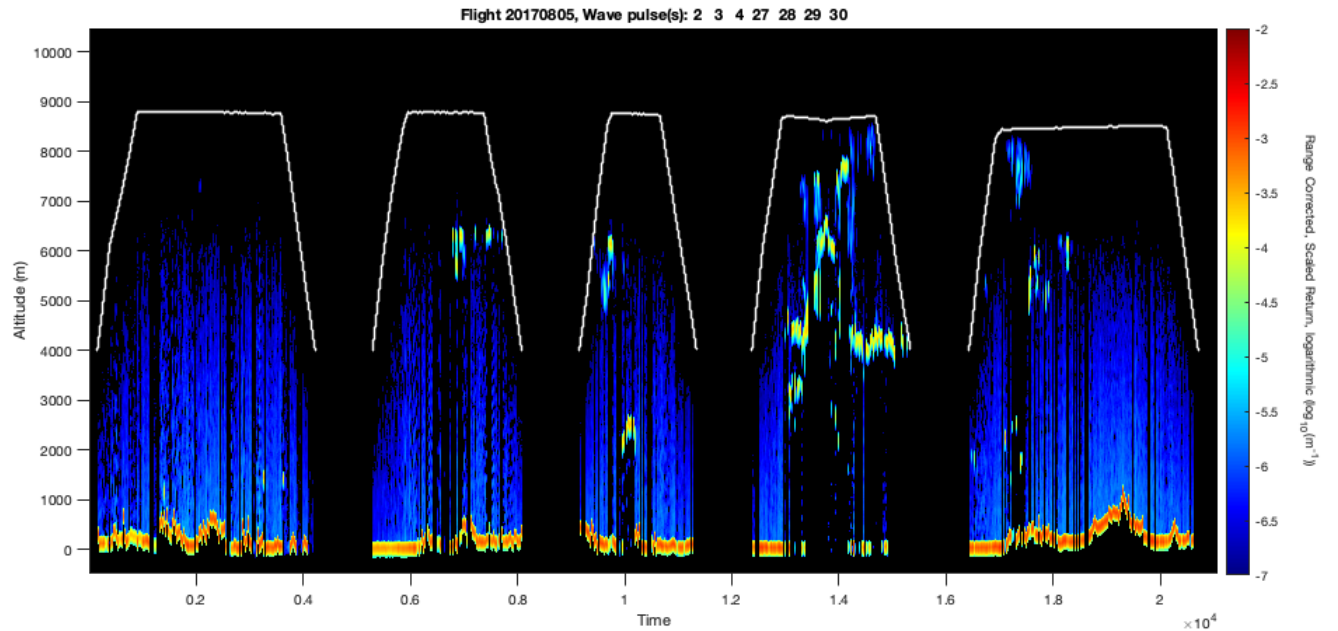
4. Science Flight, 7/31/2017



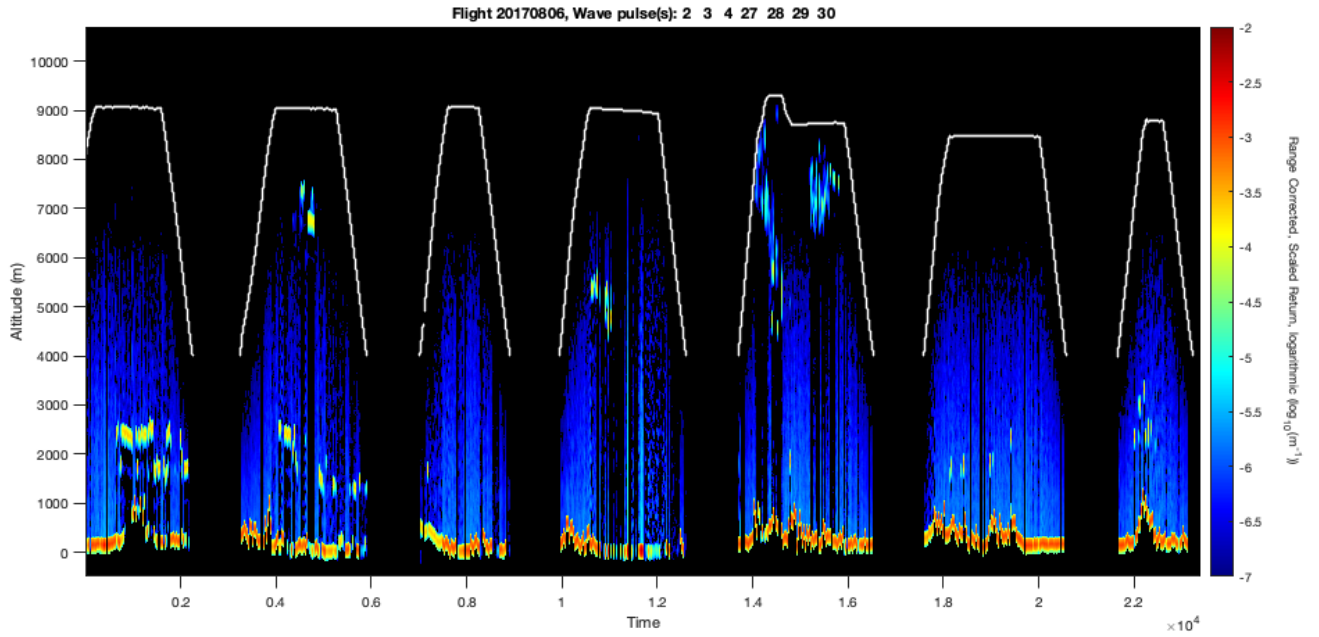
5. Science Flight, 8/3/2017



6. Science Flight, 8/5/2017



7. Science Flight, 8/6/2017



8. Science Flight, 8/8/2017

